Soft Poly(dimethylsiloxane) Elastomers from Architecture-Driven Entanglement Free Design

Li-Heng Cai, Thomas E. Kodger, Rodrigo E. Guerra, Adrian F. Pegoraro, Michael Rubinstein,* and David A. Weitz*

Poly(dimethylsiloxane) (PDMS) elastomers are widely used in both industry and research; for example, they are contained in personal care products, applied as sealants, and used as materials for microfluidic devices and stretchable electronics.[1,2] PDMS elastomers are typically formed by crosslinking entangled linear polymers; such conventional elastomers are intrinsically stiffer than a threshold value set by the density of entanglements that act as effective crosslinks. Making PDMS elastomers softer would allow their deformation with less energy, enabling uses that require them to easily comply with the shape of objects they contact, broadening potential applications. To make the elastomer softer, the density of crosslinks must be lowered; this goal can be easily achieved by swelling the elastomer with solvent. However, the solvent may leach out; moreover, such a PDMS gel is adhesive, which is unacceptable for applications requiring the separation of PDMS from another surface. Therefore, silicone gels intrinsically cannot be soft and nonsticky. The stickiness is lower for elastomers without solvents; however, conventional "dry" PDMS elastomers cannot have shear moduli lower than 200 kPa, the threshold set by entanglements.[3,4] A multiple-step, complex chemical synthesis circumvents this threshold by avoiding the entanglements, but results in elastomers with uncontrollable storage and loss moduli.[5] It remains a challenge to develop soft, solvent-free PDMS elastomers with controllable viscoelastic properties through a simple approach.

Here, we report soft PDMS elastomers fabricated by crosslinking bottlebrush rather than linear polymers. The bottlebrush architecture prevents the formation of entanglements, enabling soft, yet solvent-free PDMS elastomers with precisely controllable elastic moduli ranging from ca. 1 to 100 kPa, much softer than typical PDMS elastomers. We find that the elastic moduli are in excellent agreement with theoretical predictions based on classical rubber elasticity: The modulus is linearly proportional to the density of crosslinking chains. Remarkably, in addition to prescribed stiffness, the bottlebrush structure enables independent control over the loss modulus. We measure the difference in adhesiveness between the soft PDMS elastomers and commercial silicone products of similar stiffness. We find that the soft PDMS elastomers are far less adhesive due to their significantly smaller amount of uncrosslinked, free molecules as quantified by Soxhlet extraction. Importantly, the fabrication of soft PDMS elastomers is a one-step process, as easy as that for commercial silicone elastomer kits.

To overcome the intrinsic stiffness threshold of elastomers, the density of entanglements must be reduced. To this end, the entanglement molecular weight must be significantly increased. However, this requirement is impossible to meet for linear polymers in a melt, as they entangle at relatively low molecular weight.[4,6,7] An elastomer formed by such a linear polymer melt, containing both entanglements and covalent crosslinks, is illustrated by **Figure 1**A. For linear PDMS polymers the entanglement molecular weight is ca. 10^4 g mol^{-1}.[3] Unlike a linear polymer, a bottlebrush molecule has many relatively short linear side chains chemically attached to a long linear backbone.[8] Such a bottlebrush molecule can be considered a "thick" linear polymer; it has an entanglement molecular weight easily exceeding 10^7 g mol^{-1}, orders of magnitude higher than that of linear polymers (Supporting Information text). Therefore, using bottlebrush polymers rather than linear polymers enables the elimination of entanglements in a polymer melt. An elastomer formed by such a bottlebrush polymer melt, containing covalent crosslinks but no entanglements, is illustrated by Figure 1B.

We synthesize bottlebrush PDMS polymers through hydrosilylation,[9] which proceeds by the addition of silicone hydride to unsaturated vinyl groups. We use a multiple-functional linear PDMS copolymer, trimethylsiloxy terminated vinylmethylsiloxane–dimethylsiloxane, as the backbone of bottlebrush molecules; this copolymer carries about 300 methyl–vinyl siloxane units, allowing multiple hydrosilylation reactions per chain. To form a bottlebrush molecule, many monofunctional linear PDMS polymers, monohydride terminated poly(dimethylsiloxane), each carrying one terminal hydride group, are grafted to a backbone, acting as side chains. To simultaneously crosslink bottlebrush molecules, we use difunctional linear PDMS polymers, dihydride-terminated poly(dimethysiloxane), as covalent crosslinks; they bridge the backbones of bottlebrush molecules to form a network. Importantly, the copolymer structure of the backbone allows its miscibility with other PDMS polymers; half of the units in the backbone are dimethylsiloxane groups which favorably interact with other PDMS units on both the side chains and

Dr. L.-H. Cai, Dr. T. E. Kodger, Dr. R. E. Guerra,
Dr. A. F. Pegoraro, Prof. D. A. Weitz
John A. Paulson School of
Engineering and Applied Sciences
Harvard University
Cambridge
MA 02138, USA
E-mail: weitz@seas.harvard.edu
Prof. M. Rubinstein
Department of Chemistry
University of North Carolina
Chapel Hill
NC 27599-3290, USA
E-mail: mr@unc.edu

Materials Views
www.MaterialsViews.com

ADVANCED
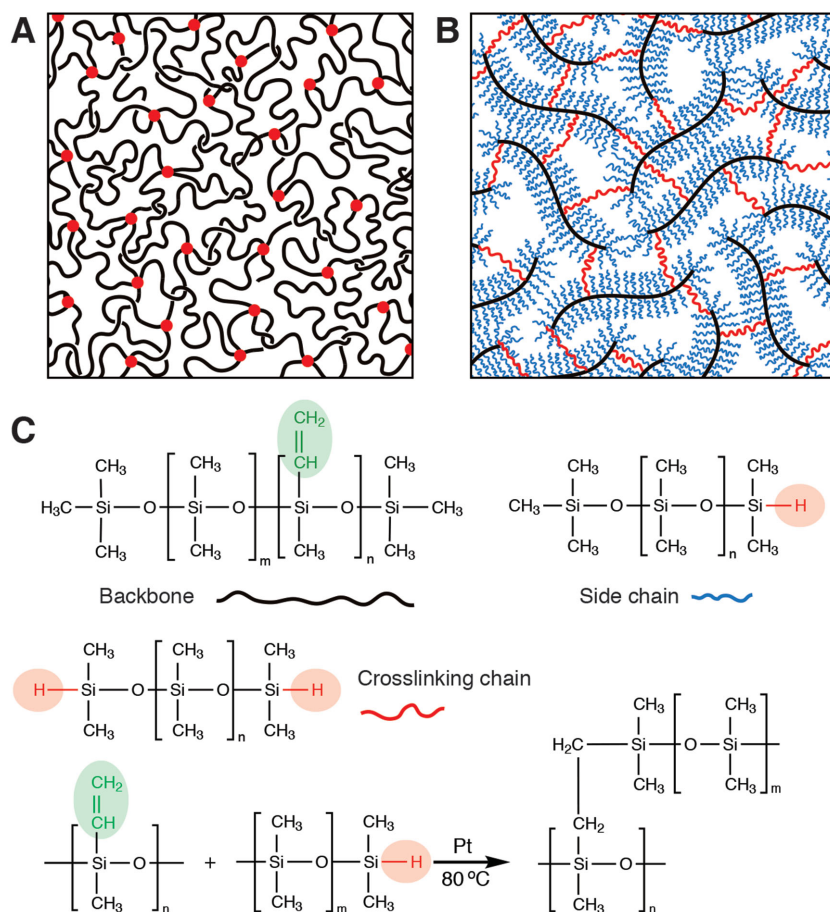MATERIALS
www.advmat.de

COMMUNICATION

Figure 1. Molecular design of soft elastomers. A) Schematic view of a conventional elastomer formed by crosslinking linear polymers: Red circles denote chemical crosslinks, and knots denote entanglements. B) Schematic view of a soft elastomer fabricated by crosslinking bottlebrush polymers: A multifunctional linear polymer chain acts as backbone (black); it is grafted by many side chains (blue), which are relatively short, monofunctional linear polymers carrying one reactive site, and crosslinking chains (red), which are difunctional linear polymers. C) Three types of precursor reactive linear PDMS polymers form the structure illustrated by (B) through hydrosilylation reactions with the aid of platinum catalyst at 80 °C.

Figure 2B and Figure S2 (Supporting Information). Therefore, we take the value of G' at the lowest frequency, 10^{-2} Hz, as the equilibrium modulus, G, of the network. Remarkably, the values of G for all elastomers formed by crosslinking bottlebrush PDMS are lower than the plateau modulus, 200 kPa, of entangled linear PDMS melts.

To explore the range of moduli achievable for soft PDMS elastomers, we vary the density of crosslinks by adjusting the number of crosslinking chains. To keep the molar ratio between vinyl and hydride groups constant at 2:1 as we increase the amount of difunctional crosslinking chains, we simultaneously reduce the number of monofunctional side chains. This method ensures the same condition for polymerization of different samples. Moreover, it ensures an excess amount of vinyl groups; this is important for completion of the crosslinking process which slows at the end of polymerization due to increases in steric hindrance from the densely grafted side chains. By tuning the concentration of crosslinking chains, we successfully produce a wide range of elastic moduli from ca. 1 to 100 kPa, as listed in **Table 1**.

To quantitatively understand the dependence of elastic moduli on concentration of crosslinking chains for soft PDMS elastomers, we apply the classic estimate for elasticity of a rubber without entanglements.[11] The equilibrium modulus G of an unentangled network is proportional to the concentration of elastically effective network strands under the assumption of affine deformation where the relative deformation of each network strand is the same as the macroscopic relative deformation imposed on the whole network. This assumption is valid when the ends of network strands are attached to a fixed elastic background. In real networks, however, the ends of network strands are attached to other network strands at crosslinks. These crosslinks are not fixed in space; instead, they fluctuate around their average positions. These fluctuations lead to reduced stretching of the network strands; as a result, the shear modulus is lower than that of an affine network. Indeed, it is described by the phantom network model: $G = k_B T (\nu - \mu)$, where k_B is the Boltzmann constant, T is absolute temperature, ν and μ are the number densities of elastically effective network strands and crosslinks, respectively.[4,12] To estimate the relation between ν, μ, and the number density of crosslinking chains, we consider a soft PDMS elastomer with on average n_{cl} fully reacted, bridging crosslinking chains per bottlebrush molecule. These difunctional crosslinking chains contribute $2n_{cl}$ crosslinks, dividing the backbone of the bottlebrush molecules into $2n_{cl} - 1$ network strands. Taking into account that the crosslinking chains themselves are network strands, there are $3n_{cl} - 1$ network strands and $2n_{cl}$
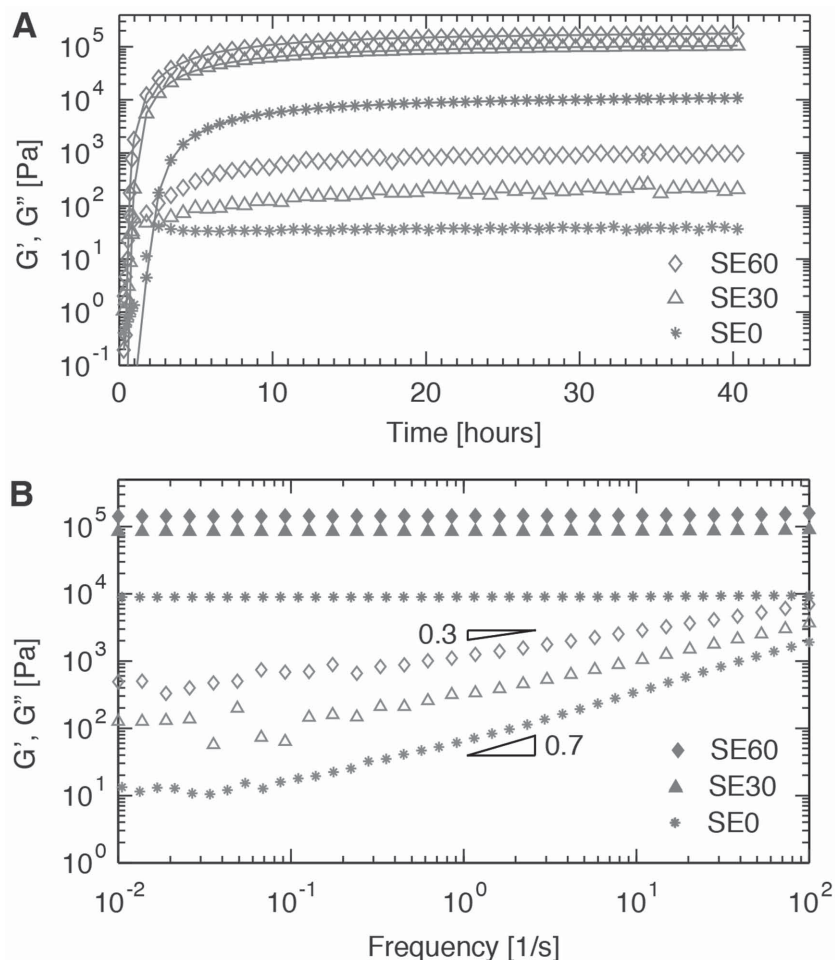
crosslinking polymers.[10] The reactions for forming and crosslinking bottlebrush polymers are both hydrosilylations, as shown in Figure 1C; this feature enables a one-step synthesis of soft PDMS elastomers.

To fabricate soft PDMS elastomers, we mix the three types of precursor linear PDMS polymers at prescribed ratios, add platinum catalyst, and elevate the temperature to 80 °C to accelerate polymerization. To determine the kinetics of polymerization, we measure the viscoelastic properties of the mixture in situ using a rheometer. The shear storage modulus increases significantly within the first few hours, exceeding the shear loss modulus, as shown in **Figure 2**A and Figure S1, Supporting Information. After about 40 h, the storage modulus reaches a stable value.

The elastomers exhibit nearly frequency-independent shear storage moduli, reminiscent of a perfect rubber.[4] Upon changing oscillatory shear frequency by four orders of magnitude, from 10^{-2} to 10^2 Hz, the amplitude of storage moduli varies by less than 10%, as shown for different samples in

COMMUNICATION

Figure 2. Rheological and mechanical properties. A) Dependence of viscoelastic properties of representative soft PDMS elastomers on curing time measured at 80 °C, 1 Hz, and a fixed strain of 0.5%. B) Frequency dependence of the storage (solid symbols, G') and loss (open symbols, G'') moduli of representative soft elastomers measured at 20 °C at a fixed strain of 0.5%. Different symbols show soft elastomers corresponding to different number of crosslinking chains per bottlebrush molecule: diamonds, SE60; triangles, SE30; stars, SE0. The recipe for each sample is listed in Table 1.

$$G = k_B T (\nu - \mu) = k_B T \rho (n_{cl} - 1) / M \qquad (1)$$

in which $\rho = 0.97$ g cm^{-3} is the density of PDMS,[13] and M is the mass of the bottlebrush molecule that includes backbone polymer, side chain, and crosslinking chain.

To test this estimate, we plot the modulus of soft elastomers as a function of $(n_{cl} - 1)/M$ as suggested by Equation (1). Consistent with the prediction of Equation (1), we find that the modulus is linearly proportional to the number of crosslinking chains per bottlebrush molecule, as shown by the solid line in the inset of **Figure 3**. The slope of this linear dependence, 2530 ± 210 Pa, is in good agreement with the predicted value, $k_B T \rho/(10^6$ g mol$^{-1}) = 2400$ Pa, corresponding to the modulus for one crosslinking chain per PDMS bottlebrush molecule of molecular weight 10^6 g mol^{-1}. However, the modulus is still finite when there is on average one crosslinking chain per brush molecule, appearing inconsistent with the prediction from Equation (1). This discrepancy suggests the possibility of difunctional chains—crosslinking chains in the commercially available monofunctional side chains. To estimate the fraction of these difunctional chains, we measure the equilibrium modulus of sample SE0 that contains only backbone polymers and side chains with molar ratio 1:150. Its modulus is $G = 8940$ Pa, which gives the number fraction of difunctional polymers in side chains: $f_{ip} = [GM/(\rho k_B T) + 1]/n_{sc} = 2.56 \times 10^{-2}$, where $n_{sc} = 150$ is the number of side chains per bottlebrush molecule. Including these difunctional chains, we calculate the effective number of fully reacted, bridging crosslinking chains per bottlebrush molecule using $n_{cl}^{eff} \equiv n_{cl} + n_{sc} f_{ip}$, and replot the modulus of soft elastomers as a function of $(n_{cl}^{eff} - 1)/M$. The replotted data are in good agreement with the classic phantom network prediction by Equation (1), $G = (2530 \pm 210$ Pa$)/(10^6$ g mol$^{-1}) \times (n_{cl}^{eff} - 1)/M$, as shown by the symbols and solid line in Figure 3.

crosslinks per bottlebrush molecule (Supporting Information text and Figure S3). Therefore, the modulus of a soft PDMS elastomer is expected to be

Table 1. Recipe for fabrication of soft PDMS elastomers presented as molar ratio of each polymer component. The mixture is polymerized with the addition of Karstedt's catalyst at concentration of 5 µL g^{-1}. Equilibrium shear storage modulus is taken as the measured value at oscillatory frequency of 0.01 Hz, temperature of 20 °C, and fixed strain of 0.5%. The sample name is abbreviated with the format of "SE#", in which "SE" stands for soft elastomer, and "#" represents the number of crosslinking chains per bottlebrush molecule, except for "L" that corresponds to long side chains.

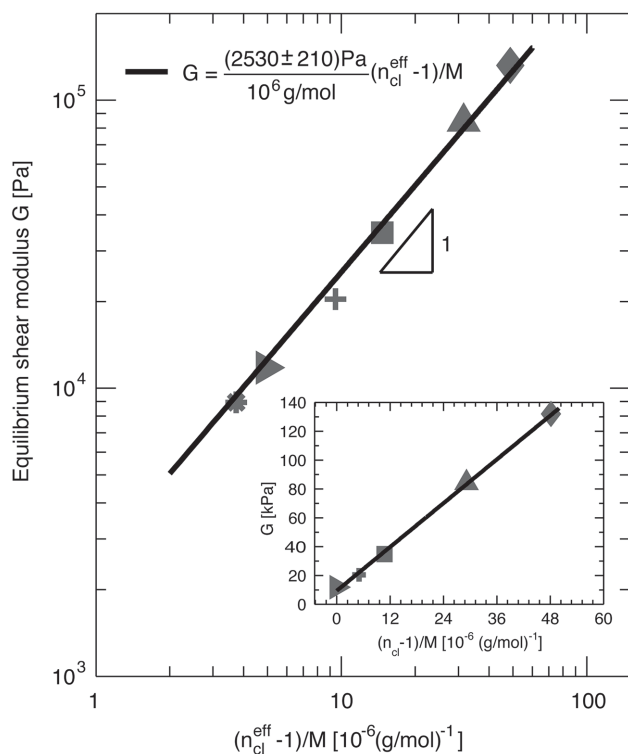| Sample name	Backbone (50 000 g mol^{-1})	Side chain (4750 g mol^{-1})	Crosslinking chain (17 200 g mol^{-1})	Extension chain (10 000 g mol^{-1})	Shear storage modulus [Pa]	Gel fraction [wt%]
SE60	1	30	60	0	132 000	93.8
SE30	1	90	30	0	84 100	–
SE10	1	130	10	0	34 700	85.6
SE5	1	140	5	0	20 400	80.3
SE1	1	148	1	0	11 800	–
SE0	1	150	0	0	8940	78.0
SEL	1	150	0	150	7430	76.2

Figure 3. Control over elastic modulus. Dependence of equilibrium shear modulus on density of crosslinking chains for soft PDMS elastomers; the equilibrium moduli are taken as the values measured at frequency of 0.01 Hz, temperature of 20 °C, and strain of 0.5%. The density of crosslinking chains is presented by $(n_{cl}^{eff} - 1)/M$, in which M is the molecular weight of a bottlebrush molecule, and n_{cl}^{eff} is the effective number of crosslinking chains per bottlebrush molecule by taking into account contributions from crosslinking chains and "impurities"—a small fraction of difunctional crosslinking chains in commercially available side chains and chain extensions. Solid line represents the best fit using Equation (1): $G = (2530\ Pa)/(10^6\ g\ mol^{-1})\ [(n_{cl}^{eff} - 1)/M]$. Inset: The density of crosslinking chains calculated based on the assumption that all crosslinking chains successfully bridge neighboring bottlebrush molecules and there are no "impurities" in side chains. The solid line represents the best fit to the data: $G = (2530\ Pa)/(10^6\ g\ mol^{-1})$ $[(n_{cl} - 1)/M] + 9370\ Pa$.

The excellent agreement between our measurements and the theoretical prediction (Equation (1)) suggests the modulus of soft PDMS elastomers can be tuned in a predictable way by changing the density of crosslinking chains. Indeed, we have successfully fabricated elastomers with shear modulus from ca. 7 to 100 kPa using solely commercially available PDMS polymers through a one-step synthesis. This simple synthesis is in contrast to fabrication of soft elastomers using a multiple-step approach, which makes it more difficult to control the network architecture; as a result, the properties of the final product are less controllable.[5,14] Moreover, the storage modulus, G', of soft PDMS elastomers is 10^2–10^3 times of the loss component, G'', at relatively low shear frequency of 1 Hz, as shown in Figure 2B. The noise in the viscous modulus, G'', at very low frequencies, <0.1 Hz, is due to the difficulty in precisely determining very small (<10^{-3}) phase angle, $\delta = \tan^{-1}(G''/G')$.[15] The magnitude of the loss modulus for soft PDMS elastomers is determined by the amount and relative molecular weight distribution of

network imperfections, which are mostly dangling chains. This correlation suggests that it may be possible to develop elastomers with controllable loss modulus by tuning the amount of network imperfections.

The ability to control the loss modulus is important for improving the fabrication of damping materials.[16] In addition, recent evidence shows that the loss modulus of the substrate is likely to play an important role in determining cell behavior.[17,18] To change the amount of network imperfections, we introduce another type of commercially available linear polymer, monovinyl-monohydride-terminated PDMS (see Experimental Section). These polymers effectively act as extension chains; they either directly graft to backbone molecules, or react with short, monofunctional side chains, forming longer side chains that can also graft to backbone molecules, as illustrated in Figure S4 (Supporting Information). Compared to sample SE0, in which the molar ratio of backbone to side chain is 1:150, in sample SEL the molar ratio of backbone, side chain, and extension chain is 1:150:150, as listed in Table 1. This recipe enables the average molecular weight of side chains in sample SEL to be three times that in sample SE0, as the molecular weight of an extension chain is twice that of a short side chain. Interestingly, compared to sample SE0, we find that the frequency-dependent loss modulus, $G''(\omega)$, for sample SEL is shifted up while maintaining a constant slope of ca. 0.75, as shown in Figure S5 (Supprtoing Information). In particular, at 1 Hz, the loss modulus increases by more than a factor of three from ca. 60 to 200 Pa. By contrast, the storage modulus of sample SEL is almost the same as that of sample SE0 as the density of crosslinking chains is nearly constant (Supporting Information text and Figure S6). Therefore, tuning the amount of side chains enables control over the magnitude of loss modulus for soft PDMS elastomers without altering its frequency-dependent behavior.

Interestingly, the loss modulus for soft PDMS elastomers is very small, nearly two orders of magnitude smaller than that of storage modulus. Nevertheless, it is clearly measurable, and exhibits a power-law dependence on frequency: $G''(\omega) \approx \omega^\alpha$. Remarkably, the value of the exponent α exhibits a strong dependence on the network elastic modulus; it increases from ca. 0.3 to 0.7 as the elastic modulus decreases from ca. 100 to 10 kPa in the frequency range of 0.1–100 Hz, as shown by the empty symbols in Figure 2B; this behavior is in sharp contrast to that of conventional elastomers with a fixed value of the exponent (Figure S7, Supporting Information). In soft PDMS elastomers, the reaction between multifunctional backbone polymers and difunctional crosslinking polymers can result in the formation of long dangling polymers that are only connected to the network framework on one end, as illustrated in Figure S8 (Supporting Information). The concentration of these long dangling polymers decreases exponentially with their length; moreover, they are constrained by the network mesh and exhibit logarithmically slow relaxation dynamics.[7] The combination of the exponential and logarithmic forms yields a power-law stress relaxation in time, and thus a power-law dependence of loss modulus on frequency (Supporting Information text).[19] The value of the exponent α describes the change in the magnitude of loss modulus with frequency: The less change of loss modulus, the smaller value of α. Indeed, the

value of α is correlated to the crosslink density of soft PDMS elastomers. As the density of crosslinks increases, the network mesh size decreases; meanwhile, the probability of forming long dangling polymers becomes smaller, thus changing the length distribution of dangling polymers. However, the length of dangling polymers decreases slightly slower compared to the network mesh size due to the presence of side chains in soft PDMS elastomers; this behavior is in contrast to conventional elastomers where both the length of dangling polymers and the network mesh size decrease in the same manner (Figure S9, Supporting Information and Supporting Information text). As a result, for soft PDMS elastomers, the dangling polymers are subjected to more constraints at higher crosslink density, and it takes a longer time for dangling polymers to relax to equilibrium. Thus, within a certain time interval, the change in the amount of relaxed dangling polymers is less, reflected by a smaller change in the magnitude of loss modulus within the corresponding frequency range. Consequently, the value of the exponent α for the frequency dependence of loss modulus decreases with the increase of crosslink density, as shown in Figure S10 (Supporting Information).

Importantly, the value of α describes the relative rather than absolute change in the magnitude of loss modulus. For instance, for soft elastomer samples SE0 and SEL, both with nearly the same crosslink density, their relative change in loss modulus is the same, reflected by the same value of $\alpha \approx 0.75$; by contrast, the absolute magnitude of loss modulus is different due to different amount of dangling polymers, as shown in Figure S5 (Supporting Information). Nevertheless, the amount of long dangling polymers in soft PDMS elastomers is very small, as evidenced by very small loss tangent, $\tan\delta = G''/G' \approx 10^{-3}$, at frequency of 1 Hz.

In addition to the effect of long dangling polymers, the exponent α may also be affected by the sol fraction, which is uncrosslinked, free polymers. By removing the sol fraction, the network mesh size becomes smaller; therefore, the dangling polymers should be subjected to more constraints from the network mesh and have slower relaxation dynamics, resulting in a smaller value of the exponent α. Indeed, the exponent α of loss modulus for a soft PDMS elastomer with storage modulus of 20 kPa decreases from 0.70 to 0.65 after the sol fraction extracted, as shown in Figure S11 (Supporting Information). Inspired by this correlation between sol fraction and the behavior of loss modulus, we also quantify the sol fraction for other soft PDMS elastomers. To do so, we perform Soxhlet extraction for 60 h using acetone/n-hexane (50:50) to remove the unreacted polymers, and measure the remaining mass after drying (see Experimental Section and Supporting Information Methods).[20] The ratio of the remaining to the initial mass is termed gel fraction. As the modulus for soft PDMS elastomers decreases from ca. 100 to 7 kPa, the gel fraction decreases from 94% (wt/wt) to 76%, as listed in Table 1; this decrease in gel fraction provides further support for the increase of the exponent of the frequency dependence of loss modulus when elastomers become softer. Interestingly, compared to commercial silicone products of similar moduli, we find that the soft PDMS elastomers have remarkably higher gel fraction. For instance, at $G \approx 7$ kPa, the gel fraction is ca. 76% for soft PDMS elastomer, which is significantly higher than ca. 50% for Sylgard

184 PDMS products. Moreover, upon a decrease in stiffness, the gel fraction only reduces slightly for soft PDMS elastomers (Table 1); by contrast, it decreases dramatically to a very small value, ca. 2%, for Sylgard 184 PDMS elastomers (Table S1, Supporting Information).

The importance of gel fraction in PDMS elastomers may be highlighted by its correlation to a material property, adhesiveness, a critical measure when involving direct contact of PDMS elastomers to objects, such as ingredients for personal care products.[21] To characterize the adhesiveness of soft PDMS elastomers, we perform adhesion measurements by bringing a spherical stainless-steel ball and a flat PDMS sample into contact.[22] The adhesive force, acting across the ball–elastomer interface, tends to deform the elastomer and thus increases the area of their contact, as illustrated schematically in **Figure 4**A. Since this deformation is opposed by the elastic restoring force, the contact area is higher for elastomers of larger adhesion, provided that they are of the same elastic modulus. For similar moduli, we find that the deformation of soft PDMS elastomers is smaller compared to commercial Sylgard 184 PDMS products and silicone gel CY 52-276, as shown in Figure 4B and Movie S1–S3 (Supporting Information). The relatively smaller deformation of soft PDMS elastomers suggests they are less adhesive compared to commercial silicone products of similar stiffness.

To quantify the adhesive properties, we measure the force applied to the flat PDMS sample as the steel ball retracts from it with a controlled velocity. This force is initially positive, due to the elastic restoration of the compressed sample. As the ball retracts, the sample becomes less compressed and thus the elastic restoration force decreases. The elastic restoration is balanced by adhesive force at a certain displacement. As the displacement, d, increases beyond this point, the adhesive force dominates and thus the force becomes negative until the ball separates from the elastomer, at which point the ball is above position d_0, the surface of the undeformed PDMS sample, as illustrated in Figure 4A. This adhesive force–dominated window is presented by the shadowed area in the force profile, as shown in Figure 4C. This area represents the work, termed fracture energy, $E_{frac}(v)$, required to separate the ball from the PDMS sample at a rate, v. Consistent with the material deformation apparent in Figure 4B, we find that E_{frac} for SE0 at $v = 10$ μm s^{-1} is about one order of magnitude lower than that for the Sylgard 184 product mixed at a ratio 1:50 and of similar modulus, as shown by the symbols close to the right in Figure 4D. Moreover, compared to another commercial silicone product, CY 52-276, the fracture energy for soft PDMS elastomer, SE0, is lower by more than two orders of magnitude at $v = 10$ μm s^{-1}.

The lower fracture energy of soft PDMS elastomers can be qualitatively understood based on energy dissipation, which accounts for the excess amount of energy to separate two surfaces in addition to surface energy. The amount of dissipated energy at a certain separation rate is lower for elastomers with lower loss modulus. Consistent with this understanding, the loss modulus of soft PDMS elastomers is much lower than that of commercial silicone products. To further explore the role of loss modulus, we measure the fracture energy at different separation rates. The fracture energy for soft PDMS elastomers
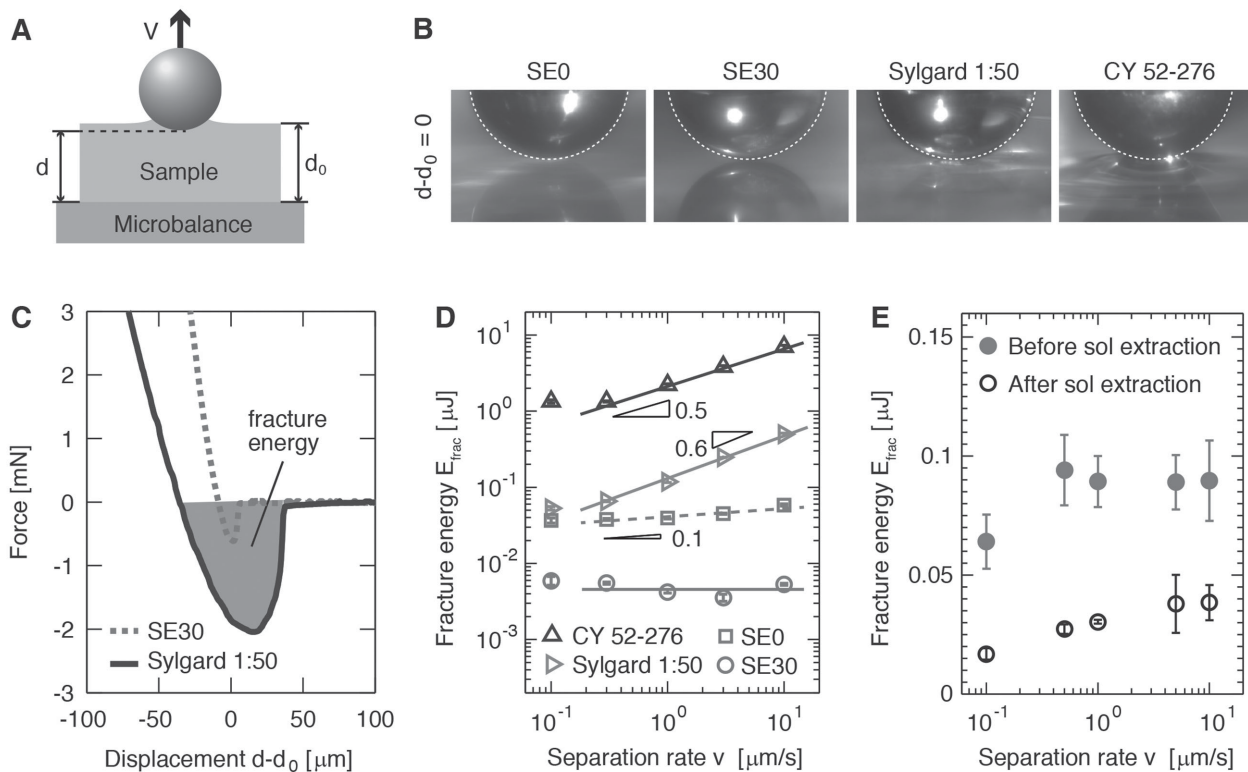
Figure 4. Adhesion. A) Schematic of adhesion test by retracting a steel ball with diameter 3.55 mm from elastomer films at a controlled velocity, v, after indentation. The adhesive force between the ball and the PDMS sample is measured by a microbalance underneath the film. B) Representative images showing the contact between the different elastomers and ball at zero displacement $d - d_0 = 0$ for the ball is retracted at 1 μm s^{-1}. C) Representative curves for retracting the ball at $v = 1$ μm s^{-1} from elastomer samples after indentation. The shadowed area represents the fracture energy required to separate the ball from the elastomer sample. D) Dependence of fracture energy on ball–film separation rate for soft PDMS elastomers (circles and squares) and commercially available silicone products (triangles). E) Fracture energy for a soft PDMS elastomer sample with modulus of 20 kPa (SE5) before and after the sol fraction extracted. Data are shown as mean ± SD with the number of samples $n \geq 3$.

is almost independent of separation rate; by contrast, the commercial silicone products have fracture energy increasing with separation rate, with a power of 0.6, as shown by the triangles and lines in Figure 4D. This result for commercial silicone products is consistent with that observed for viscoelastic polymers, which have dissipated energy typically proportional to the separation rate with a power between 0.4 and 1.[23] Indeed, the viscoelastic behavior of commercial silicone products is reminiscent of viscoelastic polymers; their loss modulus becomes comparable to the storage modulus at relatively high frequency, as shown in Figure S7 (Supporting Information). Moreover, the fracture energy for soft PDMS elastomers is lower after the sol fraction extracted, as shown in Figure 4E; this result provides direct evidence that less sol fraction corresponds to less energy dissipation and thus lower adhesiveness. Collectively, our results demonstrate that soft PDMS elastomers are different from commercial silicone products of similar stiffness in their significantly lower adhesiveness.

The independent control over storage and loss moduli could allow soft PDMS elastomers to be used as a unique substrate material to study cell behavior.[24–26] In addition to stiffness, the loss modulus is being realized as a crucial property of materials when being used as substrates to study cell–substrate interactions.[18,24,27] To demonstrate the applicability of soft PDMS

elastomers for studying cell–substrate interactions, we test the cultivation of cells on substrates made of the soft PDMS elastomers of different moduli (see the Experimental Section). We monitor the growth of MDCK epithelial and NIH/3T3 fibroblast cells and find that both cell types spread on the substrates after 24 h, and are confluent within 72 h, as shown in **Figure 5**. This result highlights that soft PDMS elastomers can be used to study cell growth and proliferation on substrates of different stiffness. Interestingly, we find that these cell types appear to proliferate faster on stiffer substrates without a change in spreading area (Figure S12, Supporting Information), contrary to similar work using hydrogel substrates.[28] This difference may be a consequence of the negligible loss modulus for soft PDMS elastomers, which is qualitatively different from hydrogels. However, further understanding of cell responses, such as spreading area, volume, proliferation rate, and differentiation on substrates made of soft PDMS elastomers is beyond the scope of this paper and will be the subject of further explorations.

We have developed soft PDMS elastomers by crosslinking bottlebrush polymers through a one-step synthesis; they have storage moduli below the lower limit of typical PDMS elastomers fabricated by crosslinking linear polymers. The stiffness of soft PDMS elastomers described here is comparable to that
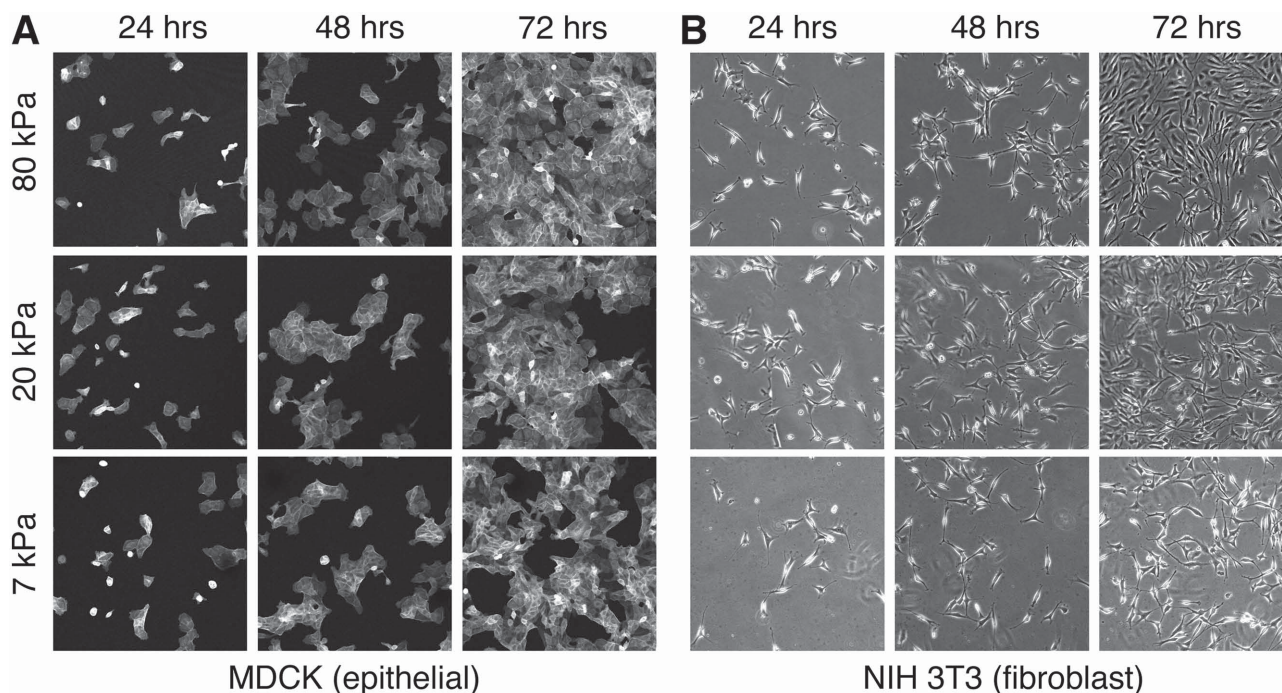
Figure 5. Biocompatibility. Fluorescence and phase contrast images showing the proliferation of A) MDCK epithelial and B) NIH/3T3 fibroblast cells at 24, 48, and 72 h on substrates formed by soft PDMS elastomers with storage moduli of 7 kPa (SEL), 20 kPa (SE5), and 80 kPa (SE30). Images are 750 μm × 750 μm.

of hydrogels;[29] moreover, in principle, extremely low moduli, <100 Pa, are achievable by using longer backbone and side chain polymers without impurities (Supporting Information text). Unlike commercial soft silicone products, soft PDMS elastomers have substantially less soluble fraction and significantly lower adhesiveness. The exceptional combination of softness and negligible adhesiveness may enable the application of soft PDMS elastomers in ultrasensitive, flexible pressure sensors.[30] In addition, the simplicity of synthesis, the commercial availability of raw ingredients, and the flexibility of choosing the backbone/side chain/crosslinking chain ratio provide a useful tool with which to precisely tune the mechanical properties of soft PDMS elastomers. This versatility, together with the biocompatibility of soft PDMS elastomers, provides an asset for industrial development of critical ingredients for personal care products,[2] designing soft materials for biomedical research and engineering,[26] and enabling materials for stretchable electronics.[31] In addition, soft PDMS elastomers offer a model system for understanding the challenging physics of unusual elasticity, dynamics, and relaxations of soft elastomers. Finally, the one-step fabrication method proposed here is not restricted to PDMS; it should be general and will enable exploration of soft elastomers made of other polymers.

Experimental Section

Reagents: All chemicals were purchased from Sigma–Aldrich (St. Louis, MO, USA) unless otherwise noted. All reactive PDMS polymers were purchased from Gelest Inc. (Philadelphia, PA, USA) and used as received. Backbone: vinylmethylsiloxane–dimethylsiloxane copolymer,

trimethylsiloxy terminated, ca. 300 vinyl groups per molecule, $M_w \approx$ 50 000 g mol^{-1} (VDT-5035). Side chain: monohydride-terminated poly(dimethylsiloxane), $M_w \approx$ 4750 g mol^{-1} (MCR-H21). Crosslinking chain: hydride-terminated polydimethysiloxane, $M_w \approx$ 17 200 g mol^{-1} (DMS-H25). Extension chain: α-monovinyl-ω-monohydride-terminated polydimethylsiloxane, $M_w \approx$ 10 000 g mol^{-1} (DMS-HV22).

Bulk Rheology: The PDMS linear polymers were mixed at a predetermined mass ratio to achieve different density of crosslinking chains. Catalyst, 2% platinum in xylene, so called Karstedt's catalyst, was added at the concentration of 5 μL g^{-1}. The mixture was cured at 80 °C for 40 h to reach a steady shear storage modulus. Rheological experiments were carried out on a stress controlled rheometer (MCR501, Anton Paar) with 50 mm plate–plate geometry at a gap of 750 μm. Frequency sweeps were performed from 10^2 to 10^{-2} Hz at 0.5% stain at temperatures 80, 20, and −20 °C. Changes in normal force due to a gap contraction with temperature were alleviated by adjusting the gap height.

Gel Fraction: To quantify the gel fraction of soft elastomers, a standard Soxhlet method was used to remove unreacted molecules in the polymerized PDMS–catalyst mixture. The extraction in acetone/n-hexane (50:50) for 60 h was performed, and then the swollen PDMS gel was dried in a vacuum oven at 80 °C for 24 h; after that the mass of PDMS did not decrease. The mass of the insoluble gel fraction was divided by the total mass before extraction and the values are listed in Table 1. The actual value of gel fraction may be larger than the measured value due to possible breakage of bonds upon swelling; swelling soft PDMS elastomers by a large extent led to a large tension along network strands that may cause bond scission.

Cell Growth: To prepare substrates for mammalian cell growth, 150 μL of the PDMS–catalyst mixture was placed in each well of a 24-well plate and polymerized at the same condition above. Then 1 mL of 1 M KOH was added to each well for 1 h to gently treat the surface of soft PDMS elastomer instead of using plasma oxidation, which can crosslink the surface of PDMS, yielding a stiffer substrate.[32] The surface was silanized by adding 500 μL of 1% (v/v) glycidyl propyl trimethoxysilane (Gelest Inc.) in ethanol, and 500 μL 1% (v/v) ammonium solution in water

sequentially to each well. After 10 min, the surface was cleaned using ethanol, and then 1× phosphate buffered saline (PBS), twice. 500 μL of 0.1 mg mL^{-1} type-1 collagen was added to each well and the plate was stored at 4 °C to prevent collagen polymerization but allow the collagen to react to the glycidyl group on the silanized PDMS surface. The above procedure was repeated with fluorescently labeled type-1 collagen and was found that the surface coverage of collagen is homogeneous and uniform in fluorescent intensity across all PDMS substrates of different stiffness. The collagen coated surfaces were washed with 1× PBS twice and then culture media: 10% fetal bovine serum (FBS) with 1% pen-strep in Dulbecco's modified Eagle medium (DMEM). 1 mL of culture media was placed in each well and warmed to 37 °C. Two cell types were used: Madin–Darby canine kidney (MDCK) epithelial cells (NBL-2, ATCC CCL-34), which had been stably transfected with plasmid pCMV LifeAct–TagGFP2 (Ibidi), and NIH/3T3 fibroblasts (ATCC CRL-1658). Trypsinized MDCK epithelial and NIH/3T3 fibroblast cells were placed on the collagen functionalized substrates at an initial concentration of ca. 20 cells mm^{-2}. Fluorescence microscopy was used to image the fluorescent actin of MDCKs and phase contrast microscopy to image NIH/3T3s. Cell growth was monitored at 37 °C over 72 h at the same location of the substrate surface; culture media was not exchanged.

Adhesion Measurement: To quantify the adhesiveness of soft PDMS elastomers, a customized adhesion apparatus was used consisting of an analytical balance (Mettler Toledo AT261) and a linear translation stage (Newport LTA-HL) remotely controlled by a motion control software (Newport Controller ESP300). The balance records mass with the rate of 1 s^{-1}, and the translation stage drives a smooth stainless-steel ball with diameter of 3.55 mm moving at a resolution of 0.0074 μm. To perform an adhesion test, the ball was lowered to a position about 100 μm above the surface of a soft PDMS elastomer sample that was placed on the balance; the sample was molded in a Petri dish with diameter of 35 mm (Nunc Petri Dishes) and has a thickness of ca. 5 mm. After that, the ball was driven at a certain rate by the linear translation stage toward the surface of soft PDMS, and the sample was indented with a distance ca. 100 μm. The ball was held at its maximum indentation, waiting 20 min for the relaxation of stress due to the compression of soft PDMS sample, and then retracted at the same rate. During the course of indentation and retraction, the force and displacement outputs were collected by customized MATLAB data acquisition software. The adhesion measurement at a certain rate was repeated at least five times; between each measurement, the steel ball was cleaned with hexane to remove possible residuals adhered to the ball surface.

Supporting Information

Supporting Information is available from the Wiley Online Library or from the author.

Acknowledgements

have filed a patent application relating to fabrication of soft elastomers from architecture-driven entanglement free design.

[1] a) G. Chandra, *Organosilicon Materials*, Springer, New York **1997**; b) *Concise Encyclopedia of High Performance Silicones*, (Eds: A. Tiwari, M. D. Soucek), John Wiley & Sons, Hoboken, NJ, USA **2014**; c) M. Andriot, S. Chao, A. Colas, S. Cray, F. deBuyl, J. DeGroot, A. Dupont, T. Easton, J. Garaud, E. Gerlach, *Silicones in Industrial Applications*, Nova Science Publishers, New York **2009**; d) Y. N. Xia, G. M. Whitesides, *Annu. Rev. Mater. Sci.* **1998**, *28*, 153.

[2] A. J. O'Lenick, *Silicones for Personal Care*, Allured Publishing, Carol Stream, IL, USA **2008**.

[3] J. E. Mark, *Physical Properties of Polymer Handbook*, Springer, New York **2006**.

[4] M. Rubinstein, R. H. Colby, *Polymer Physics*, Oxford University Press, Oxford, UK **2003**.

[5] T. Pakula, Y. Zhang, K. Matyjaszewski, H. I. Lee, H. Boerner, S. H. Qin, G. C. Berry, *Polymer* **2006**, *47*, 7198.

[6] a) W. W. Graessley, *Polymeric Liquids and Networks: Dynamics and Rheology*, Garland Science, London **2008**; b) P. G. de Gennes, *Scaling Concepts in Polymer Physics*, Cornell University Press, Ithaca, NY **1979**.

[7] S. S. Sheiko, B. S. Sumerlin, K. Matyjaszewski, *Prog. Polym. Sci.* **2008**, *33*, 759.

[8] M. A. Brook, *Organosilicon Chemistry: Synthetic Applications in Organic, Organometallic, Materials, and Polymer Chemistry*, Wiley, New York **1999**.

[9] L. Leibler, *Macromolecules* **1980**, *13*, 1602.

[10] H. M. James, E. Guth, *J. Chem. Phys.* **1943**, *11*, 455.

[11] W. W. Graessley, *Polymeric Liquids and Networks: Structure and Properties*, Garland Science, New York **2004**.

[12] H. Shih, P. J. Flory, *Macromolecules* **1972**, *5*, 758.

[13] a) D. Neugebauer, Y. Zhang, T. Pakula, S. S. Sheiko, K. Matyjaszewski, *Macromolecules* **2003**, *36*, 6746; b) K. Matyjaszewski, J. Xia, *Chem. Rev.* **2001**, *101*, 2921.

[14] S. K. Patel, S. Malone, C. Cohen, J. R. Gillmor, R. H. Colby, *Macromolecules* **1992**, *25*, 5241.

[15] K. Urayama, T. Miki, T. Takigawa, S. Kobjiya, *Chem. Mater.* **2004**, *16*, 173.

[16] a) C. S. Chen, *J. Cell Sci.* **2008**, *121*, 3285; b) A. R. Cameron, J. E. Frith, J. J. Cooper-White, *Biomaterials* **2011**, *32*, 5979.

[17] H. Mohammadi, C. A. McCulloch, *Soft Matter* **2014**, *10*, 408.

[18] J. G. Curro, P. Pincus, *Macromolecules* **1983**, *16*, 559.

[19] J. Kim, M. K. Chaudhury, M. J. Owen, *J. Colloid Interface Sci.* **2000**, *226*, 231.

[20] a) K. Moore, S. Bolduc, *J. Urol.* **2008**, *179*, 201; b) D. T. Liles, F. F. Lin, *Polym. Delivery Ther.* **2010**, *1053*, 207.

[21] K. L. Johnson, K. Kendall, A. D. Roberts, *Proc. R. Soc. London A* **1971**, *324*, 301.

[22] A. N. Gent, *Langmuir* **1996**, *12*, 4492.

[23] a) B. Trappmann, J. E. Gautrot, J. T. Connelly, D. G. T. Strange, Y. Li, M. L. Oyen, M. A. C. Stuart, H. Boehm, B. J. Li, V. Vogel, J. P. Spatz, F. M. Watt, W. T. S. Huck, *Nat. Mater.* **2012**, *11*, 642; b) J. H. Wen, L. G. Vincent, A. Fuhrmann, Y. S. Choi, K. C. Hribar, H. Taylor-Weiner, S. C. Chen, A. J. Engler, *Nat. Mater.* **2014**, *13*, 979; c) A. J. Engler, S. Sen, H. L. Sweeney, D. E. Discher, *Cell* **2006**, *126*, 677.

[24] R. J. Pelham, Y. L. Wang, *Proc. Natl. Acad. Sci. USA* **1997**, *94*, 13661.

[25] D. E. Discher, P. Janmey, Y. L. Wang, *Science* **2005**, *310*, 1139.

[26] a) A. I. Teixeira, S. Ilkhanizadeh, J. A. Wigenius, J. K. Duckworth, O. Inganas, O. Hermanson, *Biomaterials* **2009**, *30*, 4567; b) F. Chowdhury, Y. Z. Li, Y. C. Poh, T. Yokohama-Tamaki, N. Wang, T. S. Tanaka, *PLoS One* **2010**, *5*, e15655.

[27] a) M. J. Paszek, N. Zahir, K. R. Johnson, J. N. Lakins, G. I. Rozenberg, A. Gefen, C. A. Reinhart-King, S. S. Margulies, M. Dembo, D. Boettiger, D. A. Hammer, V. M. Weaver, *Cancer Cell* **2005**, *8*, 241; b) J. D. Mih, A. Marinkovic, F. Liu, A. S. Sharif, D. J. Tschumperlin, *J. Cell Sci.* **2012**, *125*, 5974.

[28] S. Naficy, H. R. Brown, J. M. Razal, G. M. Spinks, P. G. Whitten, *Aust. J. Chem.* **2011**, *64*, 1007.

[29] T. Someya, T. Sekitani, S. Iba, Y. Kato, H. Kawaguchi, T. Sakurai, *Proc. Natl. Acad. Sci. USA* **2004**, *101*, 9966.

[30] J. A. Rogers, T. Someya, Y. Huang, *Science* **2010**, *327*, 1603.

[31] G. Bartalena, Y. Loosli, T. Zambelli, J. G. Snedeker, *Soft Matter* **2012**, *8*, 673.

[32] S. Munster, L. M. Jawerth, B. A. Leslie, J. I. Weitz, B. Fabry, D. A. Weitz, *Proc. Natl. Acad. Sci. USA* **2013**, *110*, 12197.